Applied Physics Express **5** (2012) 087301
http://dx.doi.org/**10.1143/APEX.5.087301**

Molding the Acoustic Attenuation in Quasi-Ordered Structures: Experimental Realization

Vicent Romero-García[1]*, Juan Vicente Sánchez-Pérez[2], and Luis Miguel Garcia-Raffi[3]

[1]*Instituto de Investigación para la Gestión Integrada de zonas Costeras, Universitat Politècnica de València, Paranimf 1, 46730, Gandia, Valencia, Spain*
[2]*Centro de Tecnologías Físicas: Acústica, Materiales y Astrofísica, Universitat Politècnica de València, Camino de Vera s/n, 46022 Valencia, Spain*
[3]*Instituto Universitario de Matemática Pura y Aplicada, Universitat Politècnica de València, Camino de Vera s/n, 46022 Valencia, Spain*

Received June 23, 2012; accepted July 8, 2012; published online July 27, 2012

Inverse-designed scattering acoustical elements, called quasi-ordered structures (QOSs), are theoretically and experimentally reported in this work, showing their possibilities as attenuation devices. Multiobjective evolutionary algorithms together with multiple scattering theory have been used to design a distribution of vacancies in a phononic crystal in order to create a QOS with predetermined properties. This work shows the experimental realization of QOSs with both high and stable values of acoustic attenuation in a given range of frequencies, proving the performance of the optimization procedure. Molding the acoustic attenuation is one of the most important properties for the design of effective filters.

Scattering of waves inside arrangements of many scatterers has been a problem intensively analyzed in several branches of science, including electromagnetic, acoustics, or water waves. In these systems, the radiation is scattered many times producing a multiple scattering process leading to different phenomena depending mainly on the spatial distribution of the scatterers. On one hand, media with periodic spatial distribution of either dielectric properties, known as photonic crystals,[1)] or elastic properties, known as phononic crystals (PC),[2)] have attracted increasing interest in the last few years due to their particular dispersion relation. Perhaps the most well-known property of these crystals is the presence of bandgaps, ranges of frequencies where only evanescent waves can be excited in the periodic material.[3)] These systems have shown several applications in both optics[4)] and acoustics.[5)] On the other hand, the scattering of waves in the random distribution of scatterers has been increasingly studied in recent years because of the challenging fundamental problems it offers and its manifest technological importance.[6)]

From a practical point of view, physicists have progressively realized that devices with this kind of disorder offer interesting possibilities for technological applications.[7)] For example, quasicrystals are structural forms that are both ordered and nonperiodic.[8)] They form patterns that fill the whole space but lack translational symmetry. Just like crystals, quasicrystals produce modified Bragg diffraction. Where crystals have a simple repeating structure, quasicrystals are more complex. Recently, the Anderson localization of light in a perturbed periodic potential, caused by random fluctuations on a two-dimensional (2D) photonic lattice, has been experimentally observed.[9)] Florescu *et al.* have proven that, although the bandgap is a property of periodic materials, one can design 2D, isotropic, translationally disordered photonic materials of arbitrary size with large and complete bandgaps.[10)]

In this work, we design scattering acoustical elements for the control of the sound attenuation in a given range of frequencies called quasi-ordered structures (QOSs). The design procedure starts from a purely 2D PC and follows an optimization process described below, which takes into account both the phase of the dispersed waves and the full complex scattering phenomenon. We design a random distribution of vacancies in the starting crystal in such a way that the final structure, QOS, attains the prescribed attenuation properties in the given range of frequencies. Figures 1(a) and 1(b)–1(d) show the transversal cut of the starting PC and several QOSs, respectively. The starting PC is made of aluminum cylinders embedded in air with radius $r = 2\,\mathrm{cm}$, arranged in a triangular array with lattice constant $a = 6.35\,\mathrm{cm}$. The starting structure has 73 cylinders arranged in 7 rows as shown in Fig. 1(a).

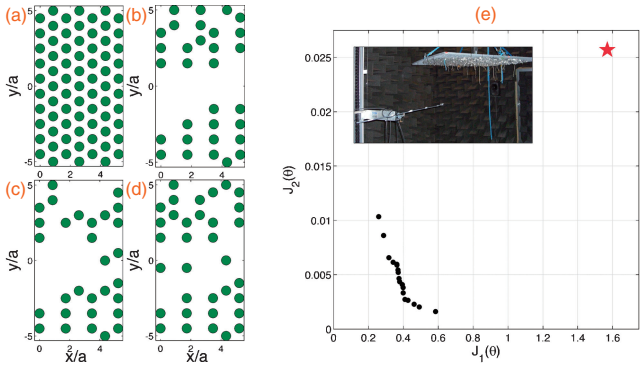

Fig. 1. (a) Cross-sectional view of the considered 2D phononic crystal made of aluminum cylinders embedded in air, with lattice constant $a = 6.35\,\mathrm{cm}$ in a triangular lattice. (b–d) Quasi-Ordered Structures. (e) Pareto front corresponding to the optimization process developed in this work. The inset shows the experimental setup.

In opposition to the quasicrystal structures, the QOSs are also nonperiodic but they cannot be considered ordered due to the random generation of vacancies. However, the random vacancies in PC have been shown as a good and efficient alternative to improve the attenuation properties of PCs.[11)] Therefore, the notion of quasi order emerges as somewhat between the periodic and the purely random structures.

The experimental validation of the designed QOS is also shown in this work. With these experiments, we prove the robustness of the inverse design described in this work. The experiments have been performed in an echo-free chamber of $8 \times 6 \times 3\,\mathrm{m}^3$ size. We use a three-dimensional robotized measurement system (3DReAMS) to move the microphone in accurate 3D trajectories inside the echo-free chamber [see inset of Fig. 1(e)]. Both the movement of the microphone and the acquisition of the temporal signal are synchronized.

*E-mail address: virogar1@gmail.com

The frequency response of the sample is obtained from the Fourier transform of the temporal signal. We build the samples hanging aluminum cylindrical scatterers on a periodic frame [inset of Fig. 1(e)]. A directional sound source GENELEC 8040A emitting continuous white noise has been used throughout the experiments.

The optimization technique followed in this work is based on the use of evolutionary algorithms (EAs),[12] which mimic biological evolution. This is made possible thanks to the nature of EAs based on populations of individuals. The good results obtained with EAs, together with their capability to handle a wide variety of problems with different degrees of complexity, explain why they are used more frequently.[13–15] Here, the multiobjective genetic algorithms (MOGAs) based on genetic algorithms have been used. Specifically, we use the ϵ-MOGA variable (ϵv-MOGA), which is an elitist multiobjective evolutionary algorithm based on the concept of ϵ-dominance.[16] Recently, multiobjective optimization algorithms have been successfully used to design different topologies of unit cell designs in periodic (infinite) structures exhibiting record values of normalized bandgap size.[17] In this work, we focus our attention on the optimization of the whole finite structures that are closer to the experimental realization than the infinite periodic systems.

The QOSs shown in this work are characterized using the vector $\boldsymbol{\theta}$, which is the chromosome of an individual in a population of ϵv-MOGA, i.e., the design variable. $\boldsymbol{\theta}$ has the information of the distribution of vacancies appearing in the QOS: each coordinate is linked with a site of the starting PC, in such a way that if the coordinate value is 1 (0), a scatterer (vacancy) appears in the corresponding linked site. ϵv-MOGA looks for QOSs showing high and stable attenuation values in a given range of frequencies $F = [\nu_1, \nu_N]$. To obtain high values of the attenuation in the range of frequencies, the algorithm minimizes the average pressure, p, in F, i.e., minimizes

$$J_1(\boldsymbol{\theta}) = \bar{p} = \sum_{j=1}^{N_\nu} \frac{|p_j(\boldsymbol{\theta})|}{N_\nu}, \tag{1}$$

where N_ν represents the number of frequencies considered in this range. On the other hand, to obtain a stable behaviour of the values of the attenuation in F, ϵv-MOGA simultaneously looks for QOSs that present minimum values of the mean deviation in this range of frequencies,

$$J_2(\boldsymbol{\theta}) = \sqrt{\frac{\sum_{j=1}^{N_\nu} (\bar{p} - |p_j(\boldsymbol{\theta})|)^2}{N_\nu^2}}. \tag{2}$$

In this work, J_1 and J_2 are simultaneously minimized in the point $(x, y) = (1, 0)$ (target point), as an example of the use of this procedure, and in the range of frequencies $F = [\nu_1 = 1400, \nu_N = 2000]$ Hz. We use $N_\nu = 30$, meaning $\Delta\nu = 50$ Hz. The values of the objective functions for the starting PC are $J_1 = 1.5688$ and $J_2 = 0.0257$ [red star in Fig. 1(e)].

The values of the pressure p have been obtained using the multiple scattering theory (MST),[18,19] which is a self-consistent method used to analyze the scattered field of an arrangement of scatterers considering all the orders of scattering. The well-known MST method derives in the following infinite system of linear equations,

$$A_{ls} - \sum_{j=1}^{N} \sum_{q=-\infty}^{q=\infty} t_{js} A_{jq} \alpha_{ljsq} = t_{ls} S_{ls}, \tag{3}$$

where A_{ls} are the coefficients of the series of Hankel functions that characterize the scattered waves. By this methodology, the acoustic pressure in the target point (x, y), for a distribution of cylinders characterized by chromosome $\boldsymbol{\theta}$, at the frequency ν, can be expressed as

$$p(\boldsymbol{\theta}, x, y, k) = p_{\text{inc}} + \sum_{l=1}^{N} \sum_{s=-\infty}^{s=\infty} A_{ls} H_{ls}(kr_l) e^{(\imath s\theta_l)}, \tag{4}$$

where $p_{\text{inc}} = \sum_s \imath^s J_s(kr) e^{\imath s\theta}$ is the incident plane wave, k is the wave number ($k = 2\pi\nu/c$), (r, θ) are the polar coordinates of the point (x, y), and (r_l, θ_l) are the polar coordinates of the point (x, y) with respect to the cylinder l. In this work, the attenuation properties have been represented using the insertion loss (IL), which is defined as

$$\text{IL} = 20 \log \frac{|p_{\text{inc}}|}{|p|}. \tag{5}$$

The solutions obtained in a multiobjective optimization process are not unique and all of them constitute the Pareto set.[20] The graphical representation of this set is known as the Pareto front, representing values of the objective functions of the optimized solutions. The key point of the problem we are dealing with is that both objectives are opposite, i.e., if one is optimized, the other is not.[21] This gives the typical picture of the Pareto front as shown in Fig. 1(e) (black dots). For comparison, the red star represents the values of the objective function for the starting PC. One can see clearly the minimization of the objective function produced by the optimization process. As an example, we discuss here the individual represented in Fig. 1(b), whose values of the objective functions are $(J_1, J_2) = (0.2587, 0.0103)$. The other QOS shown in Fig. 1 belongs also to the Pareto front shown in Fig. 1(e).

The theoretical predictions and experimental measurements of the frequency response of the QOS in comparison with the complete PC in the target point are shown in Figs. 2(a) and 2(b), respectively. The red dashed line (open red circles) represents the multiple scattering predictions (experimental results) of the IL spectrum for the complete PC; the blue line (filled blue dots) represents the multiple scattering predictions (experimental results) of the IL spectrum for the QOS. One can observe that the spectrum corresponding to the QOS presents an attenuation band at the optimized range of frequencies, and it is absent in the spectra of the starting PC. Moreover, we can observe that the values of the IL produced by the QOS inside the optimized range of frequencies present the desired results: stable (flat) and high attenuation level.

Making use of 3DReAMS, we have experimentally analyzed the IL map behind the QOS. Figures 2(d) and 2(e) show both the multiple scattering predictions and the experimental results, respectively, of the IL maps in a zone behind the structure at 1700 Hz. One can observe a good agreement between the theoretical predictions and the experimental data. One can also see that, although the optimization is done for a single point behind the structure, a neighborhood area around it presents high values of IL, and this area is preserved for the frequencies in F as it will be described below.

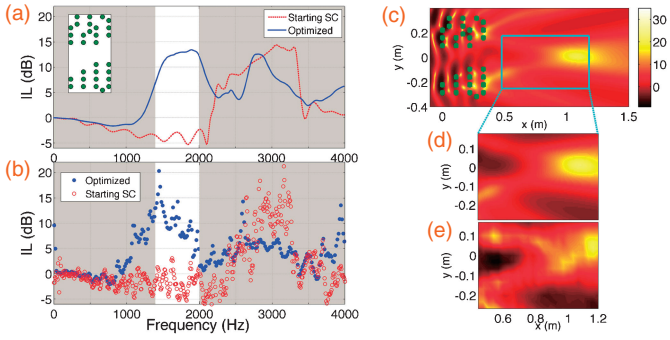

Fig. 2. Comparison between theoretical predictions and experimental results. (a) Multiple scattering simulations of the IL spectra of both complete phononic crystal (dashed red line) and QOS (continuous blue line). The white area represents the range of frequencies where the QOS is optimized. (b) Experimental results of the IL for both the complete phononic crystal (open red circles) and QOS (filled blue dots). (c) IL map at 1700 Hz for the optimized QOS. The rectangle marks the measured area in the echo-free chamber. (d) Magnified views of the multiple scattering predictions of the IL in the measured area. (e) Measured IL using 3DReAMS. Color scale represents IL.

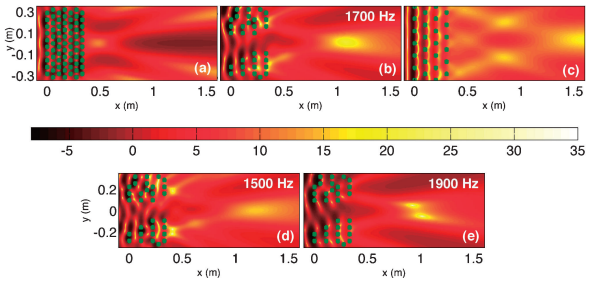

Fig. 3. Analysis of the IL behind the phononic crystal and QOS. Color scale represents the IL. IL maps for (a) complete phononic crystal at 1700 Hz, (b) optimized QOS for 1700 Hz, (c) complete phononic crystal with $a = 10$ cm, (d) QOS at 1500 Hz, and (e) QOS at 1900 Hz.

Figures 3(a)–3(c) show the theoretical comparison between the IL maps of two different complete PCs and that of the analyzed QOS, respectively. Figure 3(a) represents the IL map produced by the complete PC at 1700 Hz, which is the central frequency of F. We notice that the first bandgap of this structure appears at 3090 Hz. Thus, at 1700 Hz, there is sound propagation, and MST predicts a low attenuation around the target point. Figure 3(b) shows the IL map produced by the QOS at 1700 Hz. We observe a clear increase of the IL around the target point. For the clarity of the work, we also compare the results with the IL produced by a complete structure, the lattice constant fo which produces a bandgap at 1700 Hz. Figure 3(c) shows the IL for this complete structure with $a = 10$ cm. One can observe that the attenuation is not produced in the target point, but in other zones. Thus, the QOS can be used to create attenuation zones different than those generated by both the starting PC and the PC whose bandgap appears in F. It is worth noting that the attenuated area is preserved for all frequencies belonging to F. Figures 3(d) and 3(e) show the IL maps at 1500 and 1900 Hz, respectively, showing the high values of IL around the target point.

In summary, we have theoretically and experimentally shown that the QOSs, obtained by an inverse design technique using a multiobjective optimization process based on genetic algorithms, can be used to efficiently attenuate waves in both a given range of frequencies and a spatial region behind the filter. The scattering properties of the QOS have been theoretically and experimentally evaluated using the multiple scattering theory and a robotized acquisition system, respectively, and were found to be in good agreement. The devices shown in this work can be used for controlling the scattering properties of sound waves and this kind of system is of interest in medical applications, as, for example, ultrasonic lenses or in acoustic and mechanical engineering applications as ultrasonic actuators.

Acknowledgment This work was financially supported by the Spanish Ministry of Science and Innovation and by European Union FEDER under grants MAT2009-09438 and MTM2009-14483-C02-02. V.R.G. is grateful for the support of postdoctoral contracts of the UPV CEI-01-11. The authors would like to thank J. M. Herrero, S. García-Nieto, and X. Blasco for their discussions in ev-MOGA and their work in the control and acquisition system 3DReAMS.

1) E. Yablonovitch: Phys. Rev. Lett. **58** (1987) 2059.
2) R. Martínez-Sala, J. Sancho, J. V. Sánchez, V. Gómez, J. Llinares, and F. Meseguer: Nature **378** (1995) 241.
3) V. Romero-García, J. V. Sánchez-Pérez, S. Castiñeira Ibáñez, and L. M. Garcia-Raffi: Appl. Phys. Lett. **96** (2010) 124102.
4) H. Benisty, C. Weisbuch, D. Labilloy, M. Rattier, C. J. M. Smith, T. F. Krauss, R. M. De La Rue, R. Houdré, U. Oesterle, C. Jouanin, and D. Cassagne: J. Lightwave Technol. **17** (1999) 2063.
5) S. Yang, J. H. Page, Z. Liu, M. L. Cowan, C. T. Chan, and P. Sheng: Phys. Rev. Lett. **93** (2004) 024301.
6) M. Sahimi: *Heterogeneous Materials I: Linear Transport and Optical Properties* (Springer, New York, 2003).
7) A. Håkansson and J. Sánchez-Dehesa: Appl. Phys. Lett. **87** (2005) 193506.
8) D. Sutter-Widmer, S. Deloudi, and W. Steurer: Phys. Rev. B **75** (2007) 094304.
9) T. Schwartz, G. Bartal, S. Fishman, and M. Segev: Nature **446** (2007) 52.
10) M. Florescu, S. Torquato, and P. J. Steinhardt: Proc. Natl. Acad. Sci. U.S.A. **106** (2009) 20658.
11) V. Romero-García, J. V. Sánchez-Pérez, L. M. García-Raffi, J. M. Herrero, S. García-Nieto, and X. Blasco: Appl. Phys. Lett. **93** (2008) 223502.
12) J. Holland: *Adaptation in Natural and Artificial Systems* (MIT Press, Cambridge, MA, 1975).
13) M. I. Hussein, K. Hamza, G. M. Hulbert, R. A. Scott, and K. Saitou: Struct. Multidisciplinary Optimization **31** (2006) 60.
14) S. Halkjær, O. Sigmund, and J. S. Jensen: Struct. Multidisciplinary Optimization **32** (2006) 263.
15) M. I. Hussein, K. Hamza, G. M. Hulbert, and K. Saitou: Wave Random Complex **17** (2007) 491.
16) M. Laumanns, L. Thiele, K. Deb, and E. Zitzler: Evol. Comput. **10** (2002) 263.
17) O. R. Bilal and M. I. Hussein: Phys. Rev. E **84** (2011) 065701(R).
18) P. A. Martin: *Multiple Scattering. Interaction of Time-Harmonic Waves with N Obstacles* (Cambridge University Press, Cambridge, U.K., 2006).
19) Y. Y. Chen and Z. Ye: Phys. Rev. E **64** (2001) 036616.
20) C. Coello, D. Veldhuizen, and G. Lamont: *Evolutionary Algorithms for Solving Multiobjective Problems* (Springer, New York, 2002) 2nd ed.
21) J. M. Herrero, S. García-Nieto, X. Blasco, V. Romero-García, J. V. Sánchez-Pérez, and L. M. Garcia-Raffi: Struct. Multidisciplinary Optimization **39** (2009) 203.